

INTERNATIONAL COUNCIL FOR THE EXPLORATION OF THE SEA

C.M.1977/C:1

Hydrography Committee



Digitalization sponsored
by Thünen-Institut

This paper[†] not to be cited without prior reference to the author^{*}

THREE-DIMENSIONAL MODEL OF TIDES AND STORM SURGES

IN A SHALLOW WELL-MIXED CONTINENTAL SEA

by

Jacques C.J. NIHOUL

[†] To be published in Dynamics of Atmospheres and Ocean.

^{*} Correspondence should be addressed to :

Prof. Jacques C.J. NIHOUL,
Mécanique des Fluides Géophysiques - Environnement
Université de Liège, B6, Sart Tilman par Liège 1
B-4000 LIEGE (Belgium).

THREE-DIMENSIONAL MODEL OF TIDES AND STORM SURGES IN A SHALLOW WELL-MIXED CONTINENTAL SEA

Jacques C.J.NIHOUL

Universities of Liège and Louvain, Belgium

ABSTRACT

A three-dimensional "long waves" model is discussed for the study of tides and storm surges in a shallow well-mixed continental sea. Emphasis is placed on the North Sea where tidal and storm currents constitute the essential part of the circulation and estimates from observations in the North Sea and, more especially, the Southern Bight are used to assess the relative importance of different effects and derive a simple set of equations by which vertical profiles of tidal and storm currents can be predicted, at each points, as functions of time.

INTRODUCTION

Although depth-integrated two-dimensional models of marine circulation are now very well established, very little has been done so far in the development of three-dimensional models. This is due, in particular, to the difficulty of solving three-dimensional time dependent equations and providing appropriate boundary conditions for them.

However, in the case of long waves in a shallow sea (tides and storm surges, with a characteristic horizontal length scale much greater than the depth), horizontal turbulent diffusion and non-linear horizontal advection are usually small compared to time variations, pressure and surface elevation gradients, Coriolis acceleration and vertical turbulent diffusion. This is not true everywhere : near amphidromic points for instance (e.g. Runday 1976), typical length scales of horizontal variations of the tidal field may be much smaller than the tidal wave length. But apart from such "singular" localized area, the three-dimensional equations describing the long wave circulation in the sea reduce with a good

approximation to the classical Ekman equations where only derivatives with respect to time and the vertical coordinate appear.

This has led several authors (e.g. Jelenianski 1970, Forristall 1974) to examine the possibility of combining a two-dimensional depth-integrated model with a locally one-dimensional Ekman model to simulate the general depth-mean circulation in the sea as well as the vertical variations of velocity, turbulent stresses, etc..

In the North Sea, Nihoul and Runday (1976) have shown that a correct reproduction of tides and storm surges - including amphidromic and near coast areas - and subsequent residual currents required a non-linear depth-integrated two-dimensional model even if, in most places, the linear one-dimensional model on which the studies by Jelenianski and Forristall are based (Jelenianski 1970, Forristall 1974) could be regarded as a locally satisfactory approximation.

Models appropriate to the description of the North Sea depth-integrated circulation have been developed by several authors and are now well documented (e.g. Leendertse 1967, Heaps 1969, Nihoul and Runday 1976, Nihoul 1975, 1976, Runday 1976).

One of the main problems arising in these models is the parameterization of the bottom stress. Indeed integration over depth introduces, in the hydrodynamic equations, the surface stress and the bottom stress and, while the former can be evaluated from atmospheric data, the latter must be parameterized in terms of the mean or depth-integrated horizontal velocity introducing an empirical drag coefficient. In general, one sets (e.g. Groen and Groves 1966, Heaps 1967, Runday 1976)

$$\tau_b = -m \tau_s + D \bar{u} \|\bar{u}\| \quad (1)$$

where τ_b and τ_s are respectively the specific bottom and surface stresses (stresses divided by the specific mass of sea water) and where m and D are two empirical coefficients (D is the drag coefficient).

The parameters m and D must be adjusted not only to have the right magnitude of τ_b but also the right direction. One notes that eq. 1, if used with constant m and D , introduces a rather severe assumption on the relationship between the direction of the bottom stress and that of the mean flow velocity \bar{u} . An error at this stage might seriously affect the final prediction of the model and several authors have stressed the need of three-dimensional modelling if only to assess the limits of validity of eq. 1.

Using Ekman theory, Welander (1957) suggested that the bottom stress could be determined from the local time-histories of the wind stress and the surface slope by means of an integral operator in the form of a convolution integral. Jelesnianski (1970) used this approach to calculate bottom friction in his study of storm surges, Gedney and Lick (1972) used it to calculate steady state current profiles in Lake Erie and Forristall (1974) presented a study of hurricanes in the Gulf of Mexico based on a model using a finite difference scheme on the integrated equations of motion followed by an evaluation of convolution integrals over the sea slope and wind stress to calculate current profiles at selected points in the grid.

These very elegant studies, unfortunately, had to assume a constant vertical eddy viscosity coefficient. This assumption creates difficulties with the formulation of the bottom boundary condition (e.g. Jelesnianski 1970) and can only give a rather inadequate representation of the bottom boundary layer. Thus, having the parameterization of bottom friction particularly in mind, it has seemed interesting to try to improve the model in this respect.

In the North Sea, in typical weather conditions, the observations indicate that the vertical eddy viscosity is a function of the depth, increasing first linearly with height over the bottom and then flattening out in the upper layers following some form of parabolic curve (e.g. Bowden 1965, Roday 1976). This is obviously in relation with the existence near the sea floor of a logarithmic bottom boundary layer of which there is now ample experimental evidence (e.g. Weatherly 1977).

One of the demands upon three-dimensional models of the North Sea is thus to take into account the variations of the eddy viscosity with depth in a realistic way, respecting the linear asymptotic behaviour observed near the bottom.

The method proposed in this paper, to answer this purpose, is based on series expansions of (modified) Ekman variables in eigenfunctions of the vertical turbulent diffusivity operator. This method is somewhat similar to that used by Heaps in an earlier very attractive endeavour of three-dimensional modelling of the Irish Sea (Heaps 1972, 1976). However the setting there was different and, in particular, a constant vertical eddy viscosity coefficient was again assumed.

With this method, an analytical solution of Ekman equations (with variable eddy viscosity) can be formulated in terms of the wind stress, the vertical mean current and the associated surface elevation. A simple iteration procedure is proposed to take into account non-linear advection terms, neglected in Ekman equations, in the regions where they may be important.

The final result is a three-dimensional model of tides and storm surges composed of a depth-integrated two-dimensional model coupled, - through a new formulation of the bottom stress, in particular -, to a locally one-dimensional model by which the vertical profiles of tidal and storm currents can be predicted.

THREE-DIMENSIONAL EQUATIONS FOR TIDES AND STORM SURGES IN A WELL-MIXED SHALLOW SEA

The three-dimensional equations describing tidal and storm currents in a well-mixed (constant density) shallow sea are fairly classical. If $\underline{u} = (u_1, u_2, u_3)$ is the velocity vector, u_3 denoting the vertical component and the vertical axis pointing upwards, they can be written, (e.g. Nihoul 1975) :

$$\nabla \cdot \underline{u} = 0 \quad (2)$$

$$\frac{\partial u_1}{\partial t} + \underline{u} \cdot \nabla u_1 - f u_2 = - \frac{\partial}{\partial x_1} \left(\frac{p_a}{\rho} + g \zeta \right) + \frac{\partial}{\partial x_3} \left(\bar{v} \frac{\partial u_1}{\partial x_3} \right) \quad (3)$$

$$\frac{\partial u_2}{\partial t} + \underline{u} \cdot \nabla u_2 + f u_1 = - \frac{\partial}{\partial x_2} \left(\frac{p_a}{\rho} + g \zeta \right) + \frac{\partial}{\partial x_3} \left(\bar{v} \frac{\partial u_2}{\partial x_3} \right) \quad (4)$$

where f is twice the vertical component of the earth's rotation vector, p_a is the atmospheric pressure, ρ the specific mass of sea water, ζ the surface elevation and \bar{v} the vertical eddy viscosity.

In these equations, the quasi-static approximation has been used to eliminate the pressure, the effect of the horizontal component of the earth's rotation vector (multiplied by $u_3 \ll u_1$ or u_2) has been ignored and the horizontal turbulent diffusion of momentum has been neglected as compared with the vertical diffusion, taking into account that horizontal length scales are much larger than the depth.

If

$$x_3 = \zeta \quad \text{and} \quad x_3 = -h \quad (5) \quad (6)$$

are the equations of the free surface and the bottom, respectively, it is convenient to change variables from (x_1, x_2, x_3, t) to (x_1, x_2, ξ, t) where

$$\xi = \frac{x_3 + h}{H} \quad (7)$$

H here is the total depth, i.e.

$$H = h + \zeta \quad (8)$$

The definition of the auxiliary variable ξ is reminiscent of the well-known σ -transformation used by several authors (e.g. Freeman et al 1972, Durand 1976) but it is, in reality, only one part of it, as, for instance, one does not make use, in the following, of the σ -vertical velocity which, in the present notation, would be given by $\frac{d\xi}{dt}$.

The purpose of eq. 7 is to transform the variable range of vertical variations $(-h \leq x_3 \leq \zeta)$ into the fixed range $(0 \leq \xi \leq 1)$ which is better adapted to the determination of the eigenfunctions of the vertical turbulent diffusion operator which will be needed later.

Strictly speaking, the new variable ξ varies from some very small value $\xi_0 = \frac{z_0}{H}$ to 1, where z_0 is the so-called "rugosity length". z_0 can be visualized as the distance above the bottom where the velocity is conventionally set equal to zero, ignoring the intricate flow situation which occurs near the sea floor and willing to parameterize its effect on the turbulent boundary layer as simply as possible (e.g. Nihoul 1977). In the North Sea, the value of z_0 , which varies according to the nature of the bottom, is of the order of 10^{-3} m ($\ln \xi_0 \sim -10$) (Ronday 1976).

Although $\xi_0 \ll 1$, it cannot be set equal to zero because, as mentioned before, the linear variation of the vertical eddy viscosity near the bottom, leads to a logarithmic velocity profile which is singular at $\xi = 0$. However, one shall see in the following that the singular part of the profile can be sorted out by an appropriate change of variables, and that the new variables can be expanded in series of eigenfunctions of the vertical turbulent diffusion operator in the range $0 \leq \xi \leq 1$.

In brief, the lower limit of ξ will be taken equal to zero as long as it does not create a singularity.

Changing variables from (x_1, x_2, x_3, t) to (x_1, x_2, ξ, t) the first two terms of the left-hand sides of eqs. 3 and 4 become

$$\frac{\partial u_i}{\partial t} + A_i + B_i + S_i \quad i = 1, 2$$

where

$$A_i = u_1 \frac{\partial u_i}{\partial x_1} + u_2 \frac{\partial u_i}{\partial x_2} \quad i = 1, 2 \quad (9)$$

$$B_i = H^{-1} \frac{\partial u_i}{\partial \xi} (1 - \xi) (u_1 \frac{\partial h}{\partial x_1} + u_2 \frac{\partial h}{\partial x_2} + u_3) \quad i = 1, 2 \quad (10)$$

$$S_i = H^{-1} \frac{\partial u_i}{\partial \xi} \xi \left((u_{1s} - u_1) \frac{\partial \zeta}{\partial x_1} + (u_{2s} - u_2) \frac{\partial \zeta}{\partial x_2} - (u_{3s} - u_3) \right) \quad i = 1, 2 \quad (11)$$

and where the relation

$$\frac{\partial \zeta}{\partial t} + u_{1s} \frac{\partial \zeta}{\partial x_1} + u_{2s} \frac{\partial \zeta}{\partial x_2} = u_{3s} \quad \text{at } x_3 = \zeta \quad (12)$$

has been used, the subscripts denoting surface values.

The conditions under which the terms A, B and S - which are generated by the time derivative as well as by the non-linear advection terms - can be neglected in the case of the North Sea, are not obvious.

(The situation here is different from the studies of Jelesnianski (1970) and Foristall (1974), for instance, where the equations being linearized to begin with, a σ -type transformation cannot generate any term of importance.)

To estimate the orders of magnitude of the non-linear terms A, B and S, one must have some, even rough, idea of the vertical profile of the velocity and, for that purpose, one can presumably take Van Veen's profile ($u = u_s \xi^{0.2}$, Van Veen 1938), which is probably not too good in the immediate vicinity of the bottom but appears to reproduce satisfactorily the observations in many cases (e.g. Bowden 1965, Nihoul 1975).

Now, the function $(1 - \xi)\xi^{0.2}$ appearing in B is zero at the surface and at the bottom. Its larger values occur near the bottom (it has a maximum ~ 0.6 for $\xi \sim 0.17$). The function $\xi(1 - \xi^{0.2})$ appearing in S is more evenly distributed over the water column but it remains small everywhere (it has a maximum ~ 0.06 for $\xi \sim 0.4$).

Comparing A and S (noting that u and ζ have the same characteristic length of horizontal variations) one finds

$$\frac{S}{A} \sim \xi(1 - \xi^{0.2}) \frac{\zeta}{H}$$

Even in very shallow coastal zones, this can only be a few percents and one may reasonably neglect S as compared to A.

Dealing with long waves, one may associate to the time variations and the horizontal space variations of the velocity field a typical frequency ω ($\omega \sim 10^{-4} \sim f$) and a typical wave-length c/ω where c is the phase velocity.

Observed values of the phase velocity exceed 10m/sec even in shallow coastal areas (note that \sqrt{gH} gives 10m/sec for H only

10 meters). Maximum values of the flow velocity u are of the order of 1m/sec (e.g. Ronday 1976). The non-linear advection term A (and a fortiori S) is thus generally negligible as compared to the time derivative ; the two terms being in the ratio u/c .

This might not be true in some places, near amphidromic points, for instance where the characteristic length of horizontal variations of the velocity field could be smaller than the wave length. Its smaller value however is the grid size, because one cannot introduce in the model variations at scales which are meant to be smoothed out. Still, with a grid size of, say, 10 kms, A could be one order of magnitude larger, comparable with the time derivative. There are thus localized areas, where the non-linear terms cannot be neglected. Depth-integrated two-dimensional models cannot reproduce correctly the tide and storm surge characteristics over the whole North Sea without retaining the non-linear terms. (It can be shown that these terms are also necessary if one wants to model the residual circulation (Nihoul 1975, Nihoul and Ronday 1976)). However, if one excepts "singular" regions like amphidromic points, it seems reasonable to neglect A in the determination of the local vertical profile of the velocity.

The characteristic length of variations of the bottom topography $h(x_1, x_2)$ is not related to the wave-length c/ω . It cannot however be smaller than the grid size for the same obvious reason as before. For a 10 km grid size, each term composing B can be comparable to the time derivative. However, as shown previously, B is essentially important near the bottom where one may expect the streamlines to follow the bottom topography fairly closely. In that case, the three terms may be expected to nearly cancel each other, i.e.

$$u_1 \frac{\partial h}{\partial x_1} + u_2 \frac{\partial h}{\partial x_2} + u_3 \sim 0 \quad \text{near the bottom} \quad (13)$$

In the following, counting on a grid size of some 10 km and assuming that the departure of the left-hand side of eq.13 does not exceed 10 % of the value of the individual terms, one shall neglect B as compared to $\frac{\partial u}{\partial t}$. One should be aware, however, that, in finer grid models, for coastal studies for instance, B might be more important and, indeed, turn out to be the essential contribution of the non-linear terms to include by priority in the models.

More details about numerical values and orders of magnitude characteristic of the North Sea can be found, for instance, in (Ronday 1976).

Changing variables from x_3 to ξ , the last terms in the right-hand sides of eq. 3 and eq. 4 become

$$H^{-2} \frac{\partial}{\partial \xi} \left(\tilde{\nu} \frac{\partial u_i}{\partial \xi} \right) \quad i = 1, 2$$

Observations indicate that the eddy viscosity $\tilde{\nu}$ can be expressed as the product of a function of t , x_1 and x_2 and a function of ξ (Bowden 1965). If one sets

$$\tilde{\nu} H^{-2} = \sigma(t, x_1, x_2) \lambda(\xi) \quad (14)$$

and neglects the non-linear terms according to the discussion above, one can write eq. 3 and eq. 4 in the simple well-documented form

$$\frac{\partial u_1}{\partial t} - f u_2 = - \frac{\partial}{\partial x_1} \left(\frac{p_a}{\rho} + g\zeta \right) + \sigma \frac{\partial}{\partial \xi} \left(\lambda \frac{\partial u_1}{\partial \xi} \right) \quad (15)$$

$$\frac{\partial u_2}{\partial t} + f u_1 = - \frac{\partial}{\partial x_2} \left(\frac{p_a}{\rho} + g\zeta \right) + \sigma \frac{\partial}{\partial \xi} \left(\lambda \frac{\partial u_2}{\partial \xi} \right) \quad (16)$$

One emphasizes that these equations, although valid for the most part of the North Sea, are not applicable in localized areas where the non-linear terms are important. In such "singular" regions, however, their solution can be used as described below, to initiate an iteration process in which the non-linear terms are regarded as driving forces. The combination of eqs. 15 and 16 (or higher iteration forms of them) with a depth-integrated two-dimensional model will provide the elements of a three-dimensional model by which, at each great point, surface elevation, vertical mean current and vertical profile of the velocity can be predicted.

LOCALLY ONE-DIMENSIONAL MODEL OF THE VERTICAL VARIATIONS OF THE HORIZONTAL CURRENT

Let

$$u = u_1 + i u_2 \quad (17)$$

$$\tau = \bar{v} \frac{\partial u}{\partial x_3} = \sigma H \lambda \frac{\partial u}{\partial \xi} \quad (18)$$

$$\phi = - \frac{\partial}{\partial x_1} \left(\frac{p_a}{\rho} + g\zeta \right) - i \frac{\partial}{\partial x_2} \left(\frac{p_a}{\rho} + g\zeta \right) \quad (19)$$

eqs. 15 and 16 can be combined into the single equation

$$\frac{\partial u}{\partial t} + i f u = \phi + \sigma \frac{\partial}{\partial \xi} \left(\lambda \frac{\partial u}{\partial \xi} \right) \quad (20)$$

The forcing term ϕ is a function of t , x_1 and x_2 . Hence, although the dependence does not appear explicitly in eq. 20, u must be regarded as a function of ξ , t , x_1 and x_2 . At any given point x_1 , x_2 , eq. 20 provides a locally one-dimensional model of the vertical distribution of u as a function of time.

If τ_s and τ_b denote the values of τ at the surface and at the bottom respectively, the depth-averaged velocity \bar{u} is given by the equation

$$\frac{\partial \bar{u}}{\partial t} + i f \bar{u} = \phi + (\tau_s - \tau_b) H^{-1} \quad (21)$$

and the deviation $\hat{u} = u - \bar{u}$ is given by

$$\frac{\partial \hat{u}}{\partial t} + i f \hat{u} = \sigma \left\{ \frac{\partial}{\partial \xi} \left(\lambda \frac{\partial \hat{u}}{\partial \xi} \right) - \frac{\tau_s - \tau_b}{\sigma H} \right\} \quad (22)$$

The vertical profile of the eddy viscosity \bar{v} may be different in different circumstances but it is generally admitted that, in any case, its asymptotic behaviour for small ξ is given by

$$\bar{v} = \kappa |\tau_b|^{1/2} (x_3 + h) \quad (23)$$

where κ is an appropriate constant which, according to observations in the North Sea, may be taken as the classical Von Karman constant of turbulent boundary layer theory (e.g. Roday 1976).

Combining eqs. 14 and 23, one can see that σH must be proportional to $\kappa |\tau_b|^{1/2}$. There is no lack of generality in taking the constant of proportionality equal to 1 (the functions σ and λ are only defined by their product). Hence

$$\sigma_H = \kappa |\tau_b|^{1/2} \quad (24)$$

and

$$\lambda(\xi) \sim \xi \quad \text{for small } \xi \quad (25)$$

Changing variables to w and y defined by

$$\hat{u} = w e^{-i f t} + \frac{\tau_s}{\sigma_H} s(\xi) + \frac{\tau_b}{\sigma_H} b(\xi) \quad (26)$$

$$y = \int_0^t \sigma(v) dv \quad (27)$$

where

$$s(\xi) = \int_{\xi_0}^{\xi} \frac{\eta}{\lambda(\eta)} d\eta \quad (28)$$

$$b(\xi) = \int_{\xi_0}^{\xi} \frac{1 - \eta}{\lambda(\eta)} d\eta \quad (29)$$

eq. 22 can be written

$$\frac{\partial w}{\partial y} + \theta_s s(\xi) + \theta_b b(\xi) = \frac{\partial}{\partial \xi} \left(\lambda \frac{\partial w}{\partial \xi} \right) \quad (30)$$

where

$$\theta_\alpha = \frac{e^{i f t}}{\sigma} \left(\frac{\partial}{\partial t} + i f \right) \left(\frac{\tau_\alpha}{\sigma_H} \right) = \frac{\partial}{\partial y} \left(e^{i f t} \frac{\tau_\alpha}{\sigma_H} \right) \quad \alpha = s, b \quad (31)$$

with the boundary conditions

$$\lambda \frac{\partial w}{\partial \xi} = 0 \quad \text{at } \xi = 0 \quad \text{and } \xi = 1 \quad (32)$$

If the vertical profile of the eddy viscosity is known s and b are known functions of ξ . Eq. 30 allows then the determination of the vertical profile of the velocity in terms of σ , H , θ_s and θ_b which - at any given point x_1 , x_2 - are functions of t and thus of y .

VERTICAL PROFILE OF THE HORIZONTAL CURRENT

Introducing the Laplace transforms

$$W(a, \xi) = \int_0^\infty e^{-ay} w(y, \xi) dy \quad (33)$$

$$\Theta_{\alpha}(a) = \int_0^{\infty} e^{-ay} \Theta_{\alpha}(y) dy \quad \alpha = s, b \quad (34)$$

eq. 30 can be transformed into

$$aW + \Theta_s s(\xi) + \Theta_b b(\xi) - w_0(\xi) = \frac{d}{d\xi} \left(\lambda \frac{dW}{d\xi} \right) \quad (35)$$

with the boundary conditions

$$\lambda \frac{dW}{d\xi} = 0 \quad \text{at } \xi = 0 \quad \text{and } \xi = 1 \quad (36)$$

Let now a series of functions $f(\xi)$ ($n = 0, 1, \dots$) such that

$$\frac{d}{d\xi} \left(\lambda \frac{df_n}{d\xi} \right) = -\alpha_n f_n \quad n = 0, 1, 2, \dots \quad (37)$$

$$\lambda \frac{df_n}{d\xi} = 0 \quad \text{at } \xi = 0 \quad \text{and } \xi = 1 \quad (38)$$

The α_n 's being appropriate eigenvalues with $\alpha_0 = 0$.

It is readily seen that these functions are orthogonal on $(0, 1)$. They can be further normalized by imposing

$$\int_0^1 f_n^2 d\xi = 1 \quad (39)$$

It is tempting to seek a solution of eq. 34 in the form of a series expansion in $f_n(\xi)$.

Let thus

$$W = \sum_0^{\infty} c_n f_n(\xi) \quad (40)$$

$$w_0 = \sum_0^{\infty} \omega_n f_n(\xi) \quad (41)$$

$$s = \sum_0^{\infty} s_n f_n(\xi) \quad (42)$$

$$b = \sum_0^{\infty} b_n f_n(\xi) \quad (43)$$

The coefficients ω_n , s_n , b_n are known if $\lambda(\xi)$ and thus $s(\xi)$ and $b(\xi)$ are known. The coefficients c_n are determined by eq. 35. One finds

$$c_n = \frac{\omega_n - s_n \ominus_s - b_n \ominus_b}{a + \alpha_n} \quad (44)$$

Hence

$$w = \mathcal{L}^{-1} W = \sum_0^{\infty} \left\{ \omega_n e^{-\alpha_n y} - s_n R_n^s - b_n R_n^b \right\} f_n(\xi) \quad (45)$$

where

$$R_n^\alpha = \int_0^y \theta_\alpha(y') e^{-\alpha_n(y-y')} dy' \quad \alpha = s, b \quad (46)$$

From eqs. 37 and 38, it is readily seen that

$$\int_0^1 f_n(\xi) d\xi = 0 \quad n > 0 \quad (47)$$

and that f_0 is a constant so that the first terms in the series expansions 40, 41, 42 and 43 represent the depth-mean values of the corresponding functions.

Combining eqs. 26, 31 and 45, one then obtains

$$\hat{u} = \frac{\tau_s}{\sigma H} (s(\xi) - \bar{s}) + \frac{\tau_b}{\sigma H} (b(\xi) - \bar{b}) + \sum_1^{\infty} \left\{ \omega_n e^{-\alpha_n y} - s_n R_n^s - b_n R_n^b \right\} f_n(\xi) e^{-i f t} \quad (48)$$

Here \bar{s} and \bar{b} represent the depth-averaged values of s and b and the condition that the depth-averaged value of \hat{u} must be zero has been used to eliminate ω_0 .

By successive integrations by parts, one can write, using eq. 31

$$R_n^\alpha = \sum_{p=0}^{\infty} \left[\frac{d^p \theta_\alpha}{dy^p} \frac{e^{\alpha_n y}}{\alpha_n^{p+1}} \right]_0^y e^{-\alpha_n y} \quad \begin{array}{l} \alpha = s, p \\ n = 1, 2, \dots \end{array} \quad (49)$$

$$= \sum_{q=1}^{\infty} \left\{ \alpha_n^{-q} \frac{d^q}{dy^q} \left[\frac{e^{i f t \tau_\alpha}}{\sigma H} \right]_y - \alpha_n^{-q} e^{-\alpha_n y} \left[\frac{d^q}{dy^q} \left(\frac{e^{i f t \tau_\alpha}}{\sigma H} \right) \right]_0 \right\}$$

Using eq. 24 and typical values for the North Sea (e.g. Runday, 1976), one finds that σ may vary from 10^{-4} sec^{-1} , in cases of small currents almost reduced to residual at turning tides and weak winds, to 10^{-2} sec^{-1} in cases of large tidal currents and strong winds. The time variations of the stress and velocity fields may be characterized by a typical "frequency" $\omega \sim 10^{-4} \text{ sec}^{-1} \sim f$.

Thus

$$\frac{d}{dy} = \frac{1}{\sigma} \frac{d}{dt} \sim \frac{\omega}{\sigma} \ll 1$$

Successive differentiations with respect to y should thus, if anything, reduce the order of magnitude. The eigenvalues α_n being increasing functions of n , the factor α_n^{-q} in eq. 48 will rapidly become negligibly small as n and q increase and one foresees that in eqs. 48 and 49, only a few terms of the sums will have to be retained.

With the observed values of σ , the variable y reaches values of order 10 in less than a tidal period. One can see then that the influence of the initial conditions rapidly vanishes; the factor $e^{-\alpha_n y}$ (in eqs. 48 and 49) becoming exceedingly small.

Thus, after a short time, the essential contribution to the velocity deviation will be

$$\begin{aligned} \hat{u} = & \frac{\tau_s}{\sigma H} (s(\xi) - \bar{s}) + \frac{\tau_b}{\sigma H} (b(\xi) - \bar{b}) \\ & - \sigma^{-1} \frac{\partial}{\partial t} \left\{ \frac{e^{i f t}}{\sigma H} \left(\frac{s_1 \tau_s + b_1 \tau_b}{\alpha_1} \right) \right\} f_1(\xi) e^{-i f t} \end{aligned} \quad (50)$$

One can see that Ekman veering affects only the third term (and the other smaller terms of the sum) and is most effective when σ is the smallest (low current velocities, weak winds) as one would normally expect.

The velocity deviation given by eq. 50 must satisfy the additional requirement that the total velocity be zero at the bottom, i.e.

$$\hat{u} = -\bar{u} \quad \text{at } \xi = \xi_0 \quad (51)$$

Eq. 51 provides a relationship between τ_b , \bar{u} and τ_s . Thus the bottom stress can be parameterized in terms of the depth-mean velocity and the wind stress and it can be substituted in the depth-integrated two-dimensional model. The two-dimensional model can compute the mean velocity, the surface elevation and subsequently τ_b and σ . These in terms can be substituted in eq. 50 to yield the vertical profile of the velocity.

The only difficulty is that the solution 50 and the subsequent parameterization of τ_b are not valid everywhere. In certain parts of the North Sea, the non-linear terms A and B are not negligible. They are however not dominant and in the "singular" regions they can be included in the model by an iteration process: (i) a preliminary two-dimensional model where the bottom stress is parameterized by eq. 51 or by eq. 1 (it will be shown in the next section that it is indeed a very good approximation) can be run to compute the components of the depth-averaged velocity and their horizontal gradients, (ii) eq. 50 can be used to express the depth-dependence of the non linear terms, (iii) the combination of (i) and (ii) gives A, B and if needed S as known functions of t , x_1 , x_2 and ξ which may be added as driving forces to eqs. 21 or 22, (iv) the process can be repeated until a satisfactory convergence is obtained.

Thus, one finally achieves a three-dimensional model of tides and storm surges. The model is the superposition of a depth-integrated two-dimensional model and a locally one dimensional model where the variations of the eddy viscosity with depth is properly taken into account, the bottom friction is parameterized without excessive empiricism and the non-linear effects are taken into consideration.

The inclusion of the non-linear terms and of a variable eddy viscosity is, according to Cheng (Cheng et al 1976) a significant improvement on former models developed along the same line (e.g. Heaps 1972, 1976, Foristall 1974, Cheng 1976).

APPLICATION OF THE MODEL TO THE NORTH SEA

As pointed out before, depth-integrated two-dimensional models of tides and storm surges in the North Sea have been successfully operated for many years (e.g. Nihoul and Roday 1976). Before considering undertaking a complete new simulation using the two-dimensional model in parallel with eqs. 50 and 51, it has seemed interesting to apply the locally one-dimensional model at a certain number of grid points of the two-dimensional grid where one knew from the depth-integrated model the mean velocity, the surface elevation and the order of magnitude of the non-linear terms and where sufficient experimental data were available to determine the functional dependence of the eddy viscosity on depth.

In this first application, the selected grid points where the calculation was made were chosen in regions where the non-linear terms were negligible and the depth-variation of the eddy viscosity could satisfactorily be represented by a function of the type

$$\lambda = \xi \left(1 - \frac{1}{2} \xi\right) \quad (52)$$

which has the advantage of allowing the solution of (37) in analytical form.

As, in the existing depth-integrated models, eq. 1 is used to parameterize the bottom stress, eq. 51 is exploited in this approach as a test of consistency between the two-dimensional model at any grid point and the one-dimensional depth-dependent model at the same grid point.

The eigenfunctions and the eigenvalues corresponding to eq. 52 are found to be

$$f_n = (4n + 1)^{1/2} P_{2n}(\xi - 1) \quad (53)$$

$$\alpha_n = n(2n + 1) \quad (54)$$

where P_{2n} denotes the Legendre polynomials of even order.

Eq. 50 becomes

$$\begin{aligned} \hat{u} = & \frac{\tau_s}{\sigma H} (4 \ln 2 - 2 - 2 \ln (2 - \xi)) \\ & + \frac{\tau_b}{\sigma H} (2 - 2 \ln 2 + \ln (2 - \xi) + \ln \xi) \\ & + \sigma^{-1} \frac{\partial}{\partial t} (e^{i f t} \frac{\tau_s + 2 \tau_b}{\sigma H}) (\frac{5}{12} \xi^2 - \frac{5}{6} \xi + \frac{5}{18}) e^{-i f t} \end{aligned} \quad (55)$$

where it is understood that ξ runs from 0 to 1 everywhere except in $\ln \xi$ where its lower limit must be specifically set at ξ_0 .

At $\xi = \xi_0 \sim 0$, eq. 51 gives

$$\begin{aligned} \bar{u} = & \frac{\tau_s}{\sigma H} (2 - 2 \ln 2) + \frac{\tau_b}{\sigma H} (-\ln \xi_0 + \ln 2 - 2) \\ & - \frac{5}{18} \sigma^{-1} \frac{\partial}{\partial t} (e^{i f t} \frac{\tau_s + 2 \tau_b}{\sigma H}) e^{-i f t} \end{aligned} \quad (56)$$

Hence

$$\begin{aligned} u = & \frac{\tau_s}{\sigma H} 2 \ln \frac{2}{2 - \xi} + \frac{\tau_b}{\sigma H} (\ln \xi / \xi_0 + \ln \frac{2 - \xi}{2}) \\ & - \sigma^{-1} \frac{\partial}{\partial t} (e^{i f t} \frac{\tau_s + 2 \tau_b}{\sigma H}) \frac{5}{12} \xi (2 - \xi) e^{-i f t} \end{aligned} \quad (57)$$

Eq. 57 shows that the vertical profile of the velocity u is the result of three contributions which may be related to the wind stress, the bottom stress and the effect of the Coriolis force combined with the action of wind or bottom friction.

Taking $\ln \xi_0 = -10$ as a typical value (e.g. Roday 1976), one estimates

$$\begin{aligned} \frac{\frac{\tau_s}{\sigma H} 2 \ln \frac{2}{2 - \xi}}{\frac{\tau_b}{\sigma H} (\ln \xi / \xi_0 + \ln \frac{2 - \xi}{2})} & \sim 0.1 \frac{\tau_s}{\tau_b} \\ \frac{\sigma^{-1} \frac{\partial}{\partial t} (e^{i f t} \frac{\tau_s}{\sigma H}) \frac{5}{12} \xi (2 - \xi)}{\frac{\tau_s}{\sigma H} 2 \ln \frac{2}{2 - \xi}} & \sim 0.3 \frac{u}{\sigma} \\ \frac{\sigma^{-1} \frac{\partial}{\partial t} (e^{i f t} \frac{\tau_b}{\sigma H}) \frac{5}{12} \xi (2 - \xi)}{\frac{\tau_b}{\sigma H} (\ln \xi / \xi_0 + \ln \frac{2 - \xi}{2})} & \lesssim 0.1 \frac{u}{\sigma} \end{aligned}$$

where ω is, as before, a typical frequency of time variations ($\omega \sim 10^{-4} \text{ sec}^{-1} \sim f$).

- i) In the case of strong winds ($> 10 \text{ m/sec}$) and strong currents ($> 1 \text{ m/sec}$), τ_s and τ_b are comparable ($> 10^{-3} \text{ m}^2/\text{sec}^2$), σ can be one order of magnitude larger than ω , the essential contribution is due to bottom friction, the direct effect of the wind stress does not exceed some 10 % of the former and there is no noticeable Ekman veering. This will be a fortiori true in the case of strong (tidal) currents and weak winds.
- ii) In the case of strong winds but relatively moderate currents related to residual and wind-induced circulations at slack tide, the effects of wind and bottom friction may become comparable. The Ekman veering will however remain rather limited as the ratio ω/σ will presumably still be smaller than 1.
- iii) In the case of weak wind and small currents (almost reduced to residuals at slack tide), ($\tau_s \sim \tau_b \sim 10^{-5}$) the essential contribution remains related to the bottom stress, σ may be comparable to ω and both the wind stress and the Coriolis force can produce a 10 % deviation of the vertical profile of velocity.

Thus, in a shallow continental sea like the North Sea where tides are omnipresent and can reach velocities of the order of 1 m/sec or more, one expects that, during a substantial fraction of the tidal period, Coriolis effects may be neglected and eq. 56 can be written, in first approximation,

$$\bar{u} \sim \frac{\tau_s}{\sigma H} (2 - 2 \ln 2) + \frac{\tau_b}{\sigma H} (-\ln \xi_0 + \ln 2 - 2) \quad (58)$$

Moreover, the numerical coefficient of the first term being approximately 0.1 of the coefficient of the second term, eq. 24 may be written

$$(\sigma H)^2 = \kappa^2 |\tau_b| \sim \frac{\sigma H |\bar{u}| \kappa^2}{-\ln \xi_0 + \ln 2 - 2} \quad (59)$$

or

$$\sigma_H \sim \frac{|\bar{u}| \kappa^2}{-\ln \xi_0 + \ln 2 - 2} \quad (60)$$

Combining with eq. 58, one gets

$$\tau_b \sim -m \tau_s + D \bar{u} |\bar{u}| \quad (61)$$

or, equivalently

$$\tau_b \sim -m \tau_s + D \bar{u} \|\bar{u}\| \quad (61')$$

where

$$m = \frac{2 - 2 \ln 2}{-\ln \xi_0 + \ln 2 - 2} \sim 0.07$$

$$D = \frac{\kappa^2}{(-\ln \xi_0 + \ln 2 - 2)^2} \sim 2.11 \cdot 10^{-3}$$

for $\ln \xi_0 \sim -10$

Eq. 61 is identical with the empirical formula 1. Moreover the numerical values of the coefficients m and D predicted by the model appear in close agreement with the empirical coefficients used in success in practice ($m \sim 0.1$, $D \sim 2 \cdot 10^{-3}$, Roday 1976).

The empirical bottom friction law 1 would thus seem to be valid except perhaps for a fraction of time at tide reversal. Whether this is sufficient to affect significantly the predictions of a depth-integrated model can be judged by the test of consistency: the mean velocity \bar{u} calculated by the depth-integrated model, using eq. 1, must be the same as the mean velocity \bar{u} given by eq. 56.

This proved to be the case at all points where the calculation was made. Only a slight difference was observed and this occurred, as expected at tide reversal.

Figures 1-5 give, in illustration, the results of the computation at the point $52^\circ 30' N$, $3^\circ 50' E$ under strong wind conditions where the depth-integrated model provided the following estimates

$$\begin{aligned} \|\bar{u}\| &\lesssim 0.7 \text{ m sec}^{-1} & ; & & H &\sim 28 \text{ m} & ; & & Z_0 &\sim 1.8 \cdot 10^{-3} \text{ m} \\ D &\sim 2.2 \cdot 10^{-3} & ; & & \|\tau_s\| &\lesssim 2 \cdot 10^{-4} \text{ m}^2 \text{ sec}^{-2} \end{aligned}$$

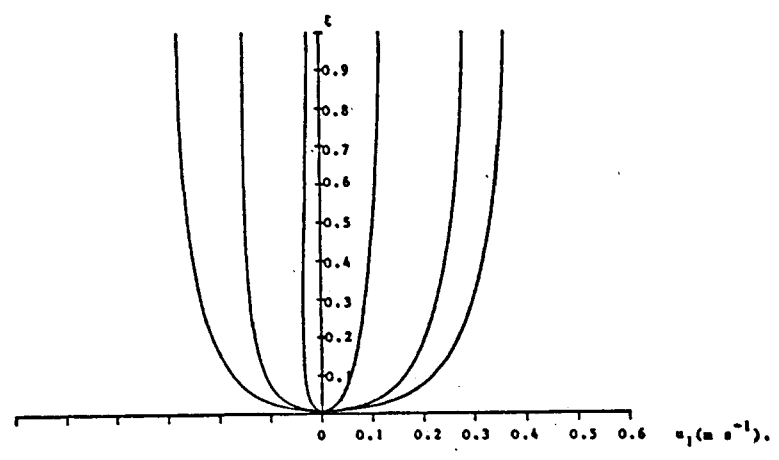


FIG. 1.

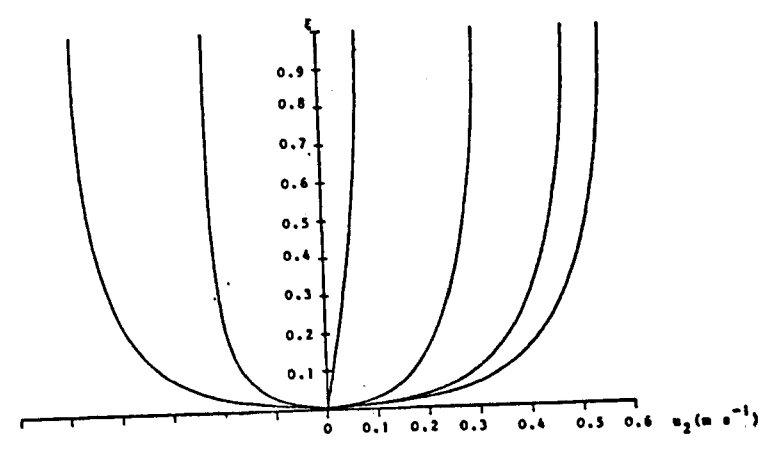


FIG. 2.

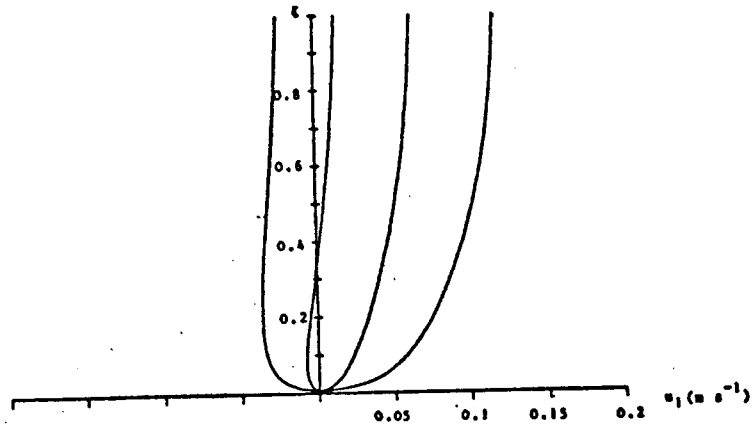


FIG. 3.

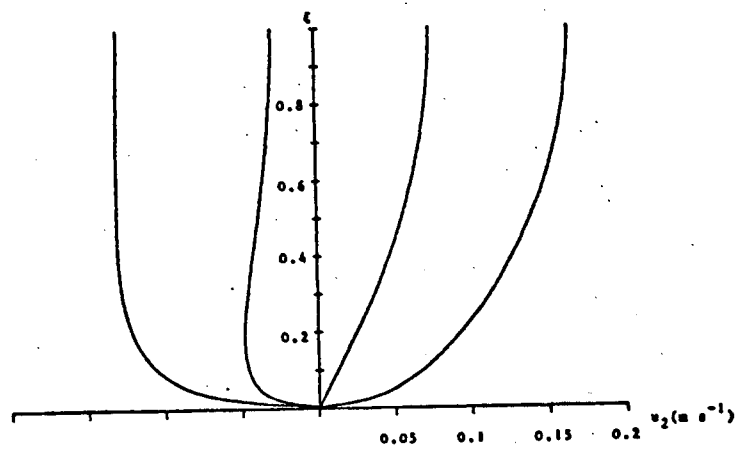


FIG. 4.

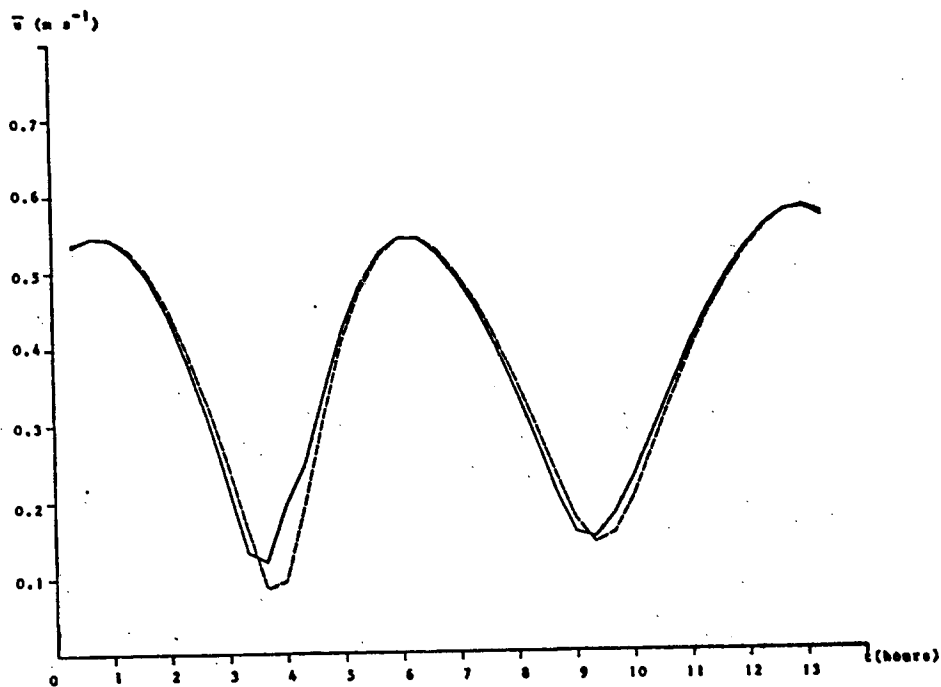


FIG. 5.

Figs. 1 and 2 show the time evolution over half a tidal period of the vertical profiles of, respectively, the northern and the eastern components of the horizontal velocity vector. The curves from left to right are vertical profiles computed at one hour interval.

Figs. 3 and 4 show the same components at tide reversal. The curves from left to right are vertical profiles computed at a 20 minutes interval. One can see, on Fig. 3 the indication of a reverse flow in the bottom layer.

Fig. 5 shows a comparison between the mean velocity computed by eq. 56 and by the two-dimensional depth-integrated model. A very good agreement is found except perhaps at minimum flow velocity associated with tide reversal.

REFERENCES

- Bowden K.F., 1965, Horizontal mixing in the sea due to a shearing current, *J. Fluid Mech.*, 21, 83-95.
- Cheng R.T., 1976, ASCE Nat. Water Res. Convent., San Diego, Preprint Paper n° 2692.
- Cheng R.T., Powell T.M. and Dillon T.M., 1976, Numerical models of wind-driven circulation in lakes, *Appl. Math. Modelling*, 1, 141-159.
- Durance J.A., 1976, A three dimensional numerical model of tidal motion in a shallow sea, *Mém. Soc. Sc. Lg.* 10, 125-132.
- Freeman N. G., Hale A.M. and Danard M.B., 1972, A modified Sigma Equations' Approach to the numerical modelling of great lakes hydrodynamics, *J. Geophys. Res.*, 77, 1050-1060.
- Forristall G.Z., 1974, Three-dimensional structure of storm-generated currents, *J. Geophys. Res.* 79, 2721-2729.
- Gedney R.T. and Lick W., 1972, Wind-driven currents in Lake Erie, *J. Geophys. Res.* 77, 2715-2723.
- Groen P. and Groves G.W., 1966, *Surges in The Sea* vol. 1, edited by N. Hill, Interscience Publishers, Wiley N.Y., 611-646.
- Heaps N.S., 1967, Storm surges, in *Oceano.Mar. Biol. Ann. Rev.*, edited by H. Barnes, Allan and Unwin Publ., London, 11-47.
- Heaps N.S., 1969, A two-dimensional numerical sea model, *Royal Soc. London Philos. Trans. Ser.A*, 265, 93-137.
- Heaps N.S., 1972, On the numerical solution of the three-dimensional hydrodynamical equations for tides and storm surges, *Mém. Soc. Sc. Lg.* 6, 143-180.
- Heaps N.S., 1976, On formulating a non-linear numerical model in three dimensions for tides and storm surges, in *Computing Methods in Applied Sciences*, edited by R. Glowinski and J.L. Lions, Springer-Verlag, Heidelberg 368-387.

- Jelesnianski C.P., 1970, Bottom stress time-history in linearized equations of motion for storm surges, Monthly Weather Review, 98, 462-478.
- Leendertse J.J., 1967, Aspects of a computational model for long-period water-wave propagation, Memo R.M. 5294-PR, Rand Corp. Santa Monica Calif.
- Nihoul J.C.J., 1975, Modelling of Marine Systems, Elsevier, Amsterdam.
- Nihoul J.C.J., 1976, Mathematical hydrodynamic models for the study of marine circulation and dispersion of pollutants in a shallow sea, in Computing Methods in Applied Sciences edited by R. Glowinski and J.L. Lions, Springer Verlag, Heidelberg 447-472.
- Nihoul J.C.J., 1977, Modèles Mathématiques et Dynamique de l'Environnement, Ele Liège.
- Nihoul J.C.J. and Ronday F.C., 1976, Hydrodynamic models of the North Sea, A comparative assessment, Mém. Soc. Sc. Lg. 10, 61-96.
- Ronday F.C., 1976, Modèles hydrodynamiques, Rapport Final Programme National Belge sur l'Environnement - Projet Mer, vol. 3.
- Van Veen J., 1938, Water movements in the Straits of Dover, J. du Conseil, Copenhagen 13, 7-38
- Weatherly G.L., 1977, Bottom Boundary Layer Observations in the Florida Current, in Bottom Turbulence, edited by J.C.J.Nihoul, Elsevier Amsterdam, 237-254.
- Welander P., 1957, Wind action on a shallow sea : some generalization of Ekman's theory, Tellus 9, 45-52.

FIGURE CAPTIONS

- Fig. 1 : Time evolution over half a tidal period of the vertical profile of the Northern component of the horizontal velocity vector at the point $52^{\circ}30'$ North, $3^{\circ}50'$ East. The curves from left to right are vertical profiles computed at one hour interval.
- Fig. 2 : Time evolution over half a tidal period of the vertical profile of the Eastern component of the horizontal velocity vector at the point $52^{\circ}30'$ North, $3^{\circ}50'$ East. The curves from left to right are vertical profiles computed at one hour interval.
- Fig. 3 : Vertical profile of the Northern component of the horizontal velocity vector at tide reversal. The curves from left to right are vertical profiles computed at a 20 minutes interval.
- Fig. 4 : Vertical profile of the Eastern component of the horizontal velocity vector at tide reversal. The curves from left to right are vertical profiles computed at a 20 minutes interval.
- Fig. 5 : Comparison between the mean velocity computed by the depth-integrated two-dimensional model (dashed line) and by the locally one dimensional depth-dependent model subject to the condition of zero velocity at the bottom (full line).